Med Bio Eng Comput (2007) 45:611–616
DOI 10.1007/s11517-007-0185-y

SHORT COMMUNICATION

Enhanced T-ray signal classification using wavelet preprocessing

X. X. Yin · K. M. Kong · J. W. Lim · B. W.-H. Ng · B. Ferguson · S. P. Mickan · D. Abbott

Received: 24 October 2006 / Accepted: 23 March 2007 / Published online: 21 April 2007

Abstract This study demonstrates the application of one-dimensional discrete wavelet transforms in the classification of T-ray pulsed signals. Fast Fourier transforms (FFTs) are used as a feature extraction tool and a Mahalanobis distance classifier is employed for classification. Soft threshold wavelet shrinkage de-noising is used and plays an important role in de-noising and reconstruction of T-ray pulsed signals. An iterative algorithm is applied to obtain three optimal frequency components and to achieve preferred classification performance.

Keywords Mahalanobis distance classifier · Wavelet denoising · T-rays

1 Introduction

T-rays lie in the 0.1–10 THz frequency range in the electromagnetic spectrum, and are non-invasive and non-ionising in nature. Rapid improvements in T-ray detectors and sources make it possible to image objects through optically opaque layers using T-rays [2]. Exciting advances in T-ray performance have focused on seizing the majority of existing efforts from the T-ray research community. As a result, the signal-processing aspects of measured T-ray signals have been relatively neglected [5]. However, significant performance improvements of T-ray technology-based systems can be realised by application of advanced signal processing in an appropriate manner.

The wavelet transform (WT) is a popular technique suited to the analysis of short-duration signals, especially signals with sudden and unpredictable changes that often carry the most interesting information [8]. The WT decomposes time domain signals into mixed time-frequency components, resulting in a variable tradeoff between time and frequency localisation. In comparison, classical Fourier-based techniques do not offer any possibility for such tradeoffs. For T-ray applications, wavelet techniques have predominantly been used for wavelet denoising prior to deconvolution of measured data, a technique first suggested in Mittleman et al. [7]. In this paper, we discuss the ability of the wavelet techniques to assist in the effective classification tasks, using T-ray measurement on a series of powder samples to illustrate our approach.

This paper adds to the important T-ray and wavelet application research fields by demonstrating enhanced classification of T-ray pulsed signals via the employment of wavelet-based preprocessing techniques.

1.1 A brief introduction to terahertz imaging

The current detection procedure works on a modified transmitted time-series T-ray pulsed response. T-ray time domain techniques allow the measurement of T-ray pulsed response in both amplitude and phase (time delay). The T-ray time domain response is obtained via terahertz pulsed imaging (TPI). Figure 1 illustrates a TPI setup; a 2D raster scan across the sample is used to generate T-ray images via repeated pulsed terahertz measurements.

X. X. Yin · K. M. Kong · J. W. Lim · B. W.-H.Ng · B. Ferguson · S. P. Mickan · D. Abbott (✉)
Centre for Biomedical Engineering and School of Electrical and Electronic Engineering, The University of Adelaide, Adelaide, SA 5005, Australia
e-mail: dabbott@eleceng.adelaide.edu.au

B. Ferguson
Tenix Defence Systems Pty Ltd, Technology Park, Mawson Lakes, Adelaide, SA 5095, Australia

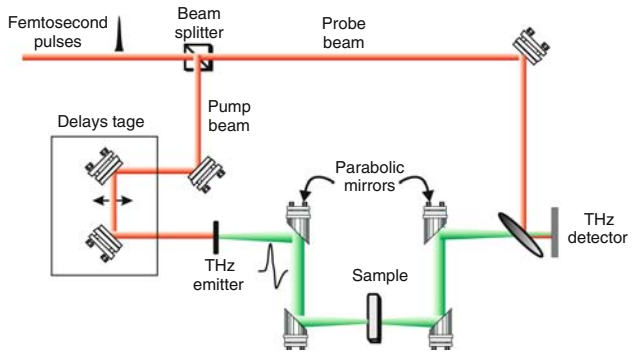

Fig. 1 Illustration of a femtosecond laser-based T-ray functional imaging system based on a pump-probe configuration. After Ferguson et al. [3]

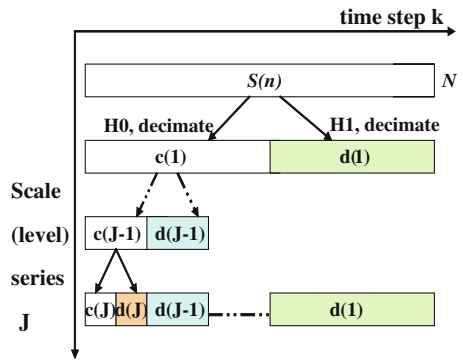

Fig. 2 The fast wavelet transform (or Mallat's algorithm) is the realisation of the DWT for 1D signals using a digital filter bank. The low- and high-pass filters indicated by $H0$ and $H1$ are decimated at each scale J; the coarse and detailed wavelet coefficients represented by **c** and **d** are functions of the time step k at scale J

An ultrafast pulsed optical laser beam is split into separate probe and pump beams. The path length of the pump beam is modulated by a delay stage, then transmitted through a chopper and an optical rectification crystal, which acts as a T-ray emitter. The T-rays produced are collimated and focused onto a sample by a pair of parabolic mirrors. The T-rays emerging from the sample are recollimated by another pair of mirrors, before being combined with the probe beam. As a result, the T-ray response and the probe beams propagate through a THz detector crystal co-linearly. The detector crystal produces an optical output, which is proportional to the T-ray response and this signal is measured with the use of an optical photodetector.

2 The methodology

2.1 Wavelet de-noising via the heuristic SURE soft threshold

The sampled transmitted T-ray signals can be analysed via the discrete wavelet transform (DWT). To realise a DWT, digital filter banks are utilised in a recursive structure to calculate WT coefficients of T-ray signals. In this paper, the DWT is implemented with Mallat's algorithm [6]. Figure 2 gives an illustration of this algorithm.

Soft threshold wavelet de-noising is known to be effective in de-noising signals [1], especially for non-stationary, pulse-like signals such as those measured using TPI techniques [2]. These are examined by the current powder experiment. The operation of soft thresholding with threshold λ on a signal X is described as follows:

$$D(X,\lambda) = \mathrm{sgn}(X)\max(0,|X|-\lambda) \quad (1)$$

The noise model used in this paper is an additive one, i.e., the measured signal X is assumed to be $X = S + N$, where S is a T-ray pulsed signal and N is the total noise.

The wavelet shrinkage de-noising in this investigation uses heuristic SURE ('heursure') soft thresholding [1], which comprises of three steps:

1. Compute DWT of the noisy signal X.
2. Perform wavelet shrinkage de-noising by applying Eq. 1 to the detail coefficients. The 'heursure' method is used for estimating the appropriate threshold λ. This hybrid method employs fixed-form threshold selection for very noisy signals, while SURE selects λ through minimisation of risk, and is used for removing high levels of noise.
3. Compute inverse WT on the modified wavelet coefficients to reconstruct the de-noised T-ray pulsed signals.

2.2 Deconvolution

As mentioned before, the combined procedure of wavelet denoising and deconvolution assumes an important role in removing system responses and noise signals for the current experiment. There are three steps involved for the recognition of target measurement: (1) the sample pulse, or T-ray response through the sample, and a reference pulse, or the T-ray response through an empty holder, are measured and denoised using the above procedure; (2) fast Fourier Transformation is conducted on both measured sample and reference responses; (3) the sample spectral response is divided from T-ray reference pulses by the system frequency response. The resultant spectrum is representative of the sample, with effects of noise and system response (i.e., empty holder) removed.

2.3 Feature extraction

Feature extraction is an important step in all classification problems. The objective of feature extraction is to obtain

the critical features from the T-ray signals to facilitate good classification performance. In this paper, the input features to the classifier are the heuristic SURE soft threshold shrinkage denoised amplitude and deconvolved phase frequency coefficients from the seven classes of T-ray data for different samples.

To reduce the dimensionality and to simplify the modeling computations, an iterative algorithm is proposed to identify a subset of the three available frequency components with optimal classification accuracy. We used frequencies up to 1.5 THz in order to keep linear phases for the extracted features. Figure 3 shows several mesaured waveforms and Fig. 3 shows the phase plot corresponding to one of those waveforms.

2.4 Classification

An important consideration in real-world detection problems is to test the ability of the classifier to accurately classify powders at the different sample thicknesses at which the classifier is trained.

In this paper, the classifier used is chosen to be a Mahalanobis distance classifier [9]. The Mahalanobis distance is defined as the distance from a feature vector $\mathbf{x}$ to the mean vector $\mathbf{m_i}$ of class i [9]. Mathematically, this distance is defined as,

$$d_i(\mathbf{x}) = \sqrt{(\mathbf{x} - \mathbf{m_i})^{\mathrm{T}} C^{-1} (\mathbf{x} - \mathbf{m_i})} \quad (2)$$

where C is the covariance matrix corresponding to the ensemble of all feature vectors $\{\mathbf{x}\}$. The minimum Mahalanobis distance is then calculated to select the sample class for any feature vector $\mathbf{x}$. This classifier design is validated by a leave-one-out error estimator, to be discussed in Sect. 2.5.

To validate the effectiveness of wavelet shrinkage denoising, leading to the enhanced ability of the classifier to classify powders, several different powder samples are tested. The current powder experiment is to detect powders inside envelopes, where six different powder samples are taped onto a sheet of paper and then put inside an envelope. The traditional scanning imaging system is used to obtain a 2D THz image of the sample. This imaging system allows differing scattering paths and minor variations in powder thickness and density to be observed. Typically, a 1D image is sufficient (i.e., raster scan in only one direction), and a 51 pixel image (with a 100 μm spatial interval for one pixel) is acquired. For this experiment, seven different powder samples were tested, which include: (1) wheat flour, (2) baking soda, (3) sucrose crystals, (4) finely powdered sucrose, (5) salt, and (6) talcum powder. A seventh trace acts as control data and is obtained with an empty envelope. Samples of three different thicknesses: 2, 3 and 4 mm, for each powder was prepared. The T-ray responses of seven powder samples in the time domain are demonstrated in Fig. 3; these measurements were obtained from the 3 mm samples.

2.5 Leave-one-out error estimator

The leave-one-out error estimator is a form of non-parametric error estimation and plays an important role in validation for pattern recognition problems. It evaluates each unknown feature vector and then produces a basis to evaluate classifier designs [4]. Under the leave-one-out error estimation procedures, all the N samples $X_j^{(i)}$, $j = 1, ..., N$ from class i are tested using a nonparametric classifier, in our case, a Mahalanobis distance classifier, trained on N–1 samples $X_i^{(i)}$, $i = 1,..., N$–1, $i \neq j$ [4].

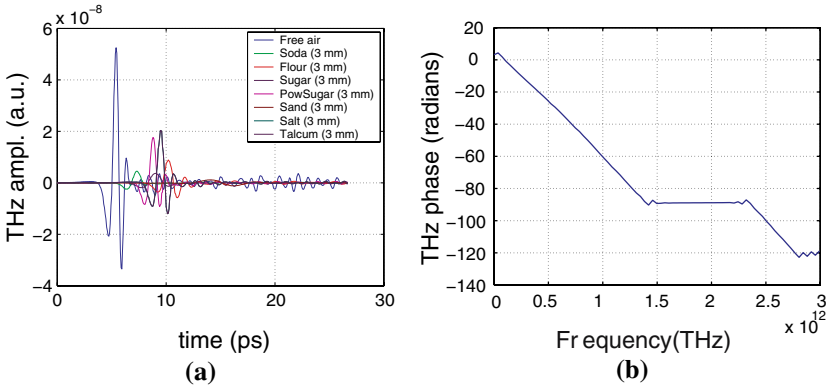

Fig. 3 Measured time domain T-ray signals and phase spectrum. **a** T-ray pulsed signals after transmission through seven different types of powder and the holder. All powders are pressed into 3 mm pellets and are as follows: baking soda, wheat flour, sucrose crystals, finely powdered sucrose, sand, table salt, and talcum powder. **b** Phase plot from the Fourier transform of the de-noised T-ray signal measured from a 3 mm soda sample

3 Results

This paper's classification experiments consist of two sets of results, which are to emphasise the comparison of performance with and without wavelet preprocessing. For both cases, two classification methods, labeled as Method (A) and Method (B), are adopted and applied to the T-ray data from seven powder samples of thicknesses 2, 3 and 4 mm. In all cases, the frequency domain amplitude and phase at discrete frequencies are used as features. With preprocessing, the T-ray data are preprocessed using the wavelet techniques detailed in section 2.

Method (A), represented in the Table 1, uses the following classification procedure. First, the Mahalanobis distance classifier was trained using the responses from 25 randomly chosen pixels of seven classes of powders at thicknesses of 2 and 4 mm. Then, the trained classifier was tested with another 25 randomly chosen pixels from all seven classes of powders, at a sample thickness of 3 mm. The computation procedure here is repeated 50 times to obtain an average accuracy. For Method (B), a leave-one-out (LOO) method is performed 51 times to validate the classifiers. That is, the classification experiment is repeated 51 times, with 50 pixels used for classifier training and one pixel for testing in each case.

In selecting the set of discrete frequencies for use in the experiments, we adopted a search approach. To limit the search scope, we considered a small number of frequencies,

Table 1 The classification accuracies for the seven types of powder samples are given

Experimental parameters	Wavelet preprocessing	Raw signals
Feature extraction		
Feature	Preprocessed amplitude and phase	Raw amplitude and phase
Method	Iterative algorithm	Iterative algorithm
Training sample thickness (mm)	2, 4	2, 4
Test sample thickness (mm)	3	3
Selected frequencies (THz)		
Comb.		
1	0.19, 0.37 and 1.38	0.22, 0.45 and 1.27
2	0.19 and 0.37	0.22 and 0.45
3	0.19 and 1.38	0.22 and 1.27
4	0.37 and 1.38	0.45 and 1.27
Method (A)		
Training vector dimensions	25 pixels	25 pixels
Test vector dimensions	25 pixels	25 pixels
Classifier	Mahalanobis	Mahalanobis
Number of tests	50 times	50 times
Averaged maximal classification accuracy (%)		
Comb.		
1	98.9	78.6
2	85.4	51.37
3	78.4	55.69
4	74.5	46.11
Method (B)		
Training vector dimensions	50 pixels	50 pixels
Test vector dimensions	1 pixel	1 pixel
Classifier	Mahalanobis	Mahalanobis
Number of tests	51 times	51 times
Average maximal classification accuracy (%)		
Comb.		
1	98.6	55.18
2	89.9	52.94
3	77.0	56.30
4	77.6	46.5

Left results column correspond to the cases with wavelet preprocessing; the rightmost column correspond to raw signals. The wavelet preprocessing, here, adopts 'heursure' soft thresholding with a Daubechies 8 (db8) wavelet at three DWT levels. The detailed subspaces are applied for the reconstruction of T-rays. Feature extraction identifies amplitude and phase feature subsets at three optimal frequencies and at the three different 2-frequency combinations. The four different frequency combinations are labelled as combinations 1, 2, 3 and 4. The training samples are taken from 2 and 4 mm measurements and the test sample has thickness of 3 mm. Two classification methods, Method (A) and Method (B) are demonstrated for the classification accuracy at the four different frequency combinations

and then evaluated different combinations of frequencies. From our search, it was found that only three optimal frequency components are sufficient to achieve very high classification accuracy after the application of de-noising preprocessing. Empirically, it was observed that adding more frequency components added to the dimensionality of the feature vectors, but the classification accuracy was not improved. The frequency selection process is performed individually for the cases of measurements with and without preprocessing, to ensure comparison between the best possible performances in both cases.

There are four feature sets formed at optimal frequency combinations that have been obtained using an iterative algorithm that examines all frequency triplets available. For the raw measurements, the three frequencies are 0.22, 0.45 and 1.27 THz; for the preprocessed signals, the three frequencies are 0.19, 0.37 and 1.38 THz. In addition to the three frequencies, classification performance of two-frequency subsets are also examined. As a result, there are four feature sets for each of the cases; these are referred to as combinations 1–4 in the results below.

3.1 Experimental results for preprocessed signals

Table 1 shows the classification steps and the corresponding classification performance mentioned earlier by applying an FFT of T-ray signals from the seven powder samples at 2 and 4 mm after heuristic SURE soft threshold shrinkage de-noising and deconvolution preprocessing. Two classification methods are compared. The classification accuracy using the leave-one-out error estimator for Method (B) is similar to the results obtained in Method (A).

In order to better understand the current classification algorithm, both the classification performance and the relative visual scatter plots after wavelet filter preprocessing were examined. Two three-dimensional amplitude scatter plots (amplitudes only) in the frequency domain are shown in Fig. 4. The seven different classes of powder samples are shown to cluster together, with just a small degree of overlap in the 3D plot. The corresponding classification accuracy reached 98.9%. To examine the effectiveness of the chosen frequencies, the three frequency features are further divided into three different subsets of two frequencies: amplitudes and phase at 0.19 and 0.37 THz, 0.19 and 1.38 THz and 0.37 and 1.38 THz. The corresponding classification accuracies obtained are 85.4, 78.4 and 74.5%, respectively. Therefore, the classification accuracy achieved with only two frequencies is at least 15% inferior to the classification accuracy achieved with three frequencies. These results are labelled in Table 1 as Method (A). Figure 4 projects the 3D scatter plot to a 2D plane with frequency components consisting of 0.19 and 0.37 THz. It is clear that Fig. 4b shows better clustering than Fig. 4a.

A leave-one-out method, labelled by Method (B), is used for comparison to Method (A). Recall that 50 pixels are randomly selected from the 51 pixels of the seven classes of powder data of 2 and 4 mm thicknesses, which are used to train the Mahalanobis distance classifier. Then the Mahalanobis distance classifier is tested by the one pixel from the seven powder samples of 3 mm thickness. The procedure is iteratively performed 51 times at each frequency combination—from combination 1 to 4 (see Table 1). The corresponding average maximal classification accuracies are calculated as 98.6, 89.9, 77 and 77.6%, respectively.

3.2 Experimental results for raw signals

For comparison, the feature sets are extracted for the classification of the raw signals via a similar procedure as described above. A set of three frequencies were selected iteratively, with the amplitude and phase at these frequencies used as features; three 2-frequency subsets are further extracted for classification experiments to justify the need for three frequencies. The averaged maximal accuracy with obtained from amplitudes and phase features at 0.22, 0.45 and 1.27 THz is 78.6%, which is 19% lower than the averaged accuracy of 98.9% obtained with pre-

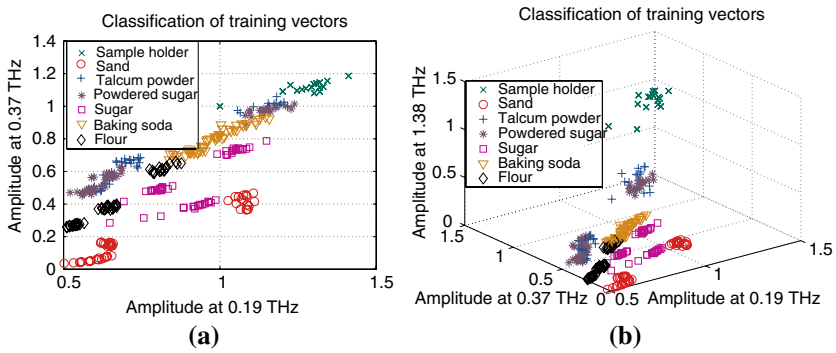

Fig. 4 Amplitude scatter plot. **a** Amplitude scatter plots at two optimal frequencies: 0.19 and 0.37 THz with a classification accuracy reaching 85.4 and 89.9% corresponding to two types of classification methods (**a**) and (**b**). **b** Amplitude scatter plots at three optimal frequencies: 0.19, 0.37 and 1.38 THz with a classification accuracy reaching 98.9%

processed signals. For the other feature sets, the averaged accuracies of the raw signals corresponding to the three 2D features are: 51.37, 55.69 and 46.11%, respectively, which are inferior to the preprocessed signals by approximately 20% across the board. Compared to the best accuracy achieved with preprocessed signals and 3D features, the 2D raw signal features were lower by 23% at best. The massive discrepancy between the two sets of signals clearly favours the use of wavelet preprocessing when performing classification experiments on T-ray signals.

When a leave-one-out error estimator, labelled as Method (b), is used to validate the classifier obtained for the raw signals, the average classification accuracies are: 55.18, 52.94, 56.30 and 46.5%, for the 3D and three 2D feature sets, respectively. There is obviously a great decrement in classification accuracy compared to the results obtained with wavelet preprocessing. The classification results of the raw signals are summarised in the last column of Table 1.

4 Conclusions

In this investigation, an improvement in classification accuracy is demonstrated by applying wavelet-based techniques in the preprocessing of T-ray pulsed signals to achieve enhanced T-ray classification. The results reveal that a higher level of accuracy can be obtained after implementing heuristic SURE wavelet shrinkage de-noising and deconvolution prior to classification. Furthermore, the classification accuracy and the visual quality of the scatter plots are demonstrated.

References

1. Donoho DL (1995) De-noising by soft thresholding. IEEE Trans Inf Theory 41(3):613–627
2. Ferguson B, Abbott D (2001) Wavelet de-noising of optical terahertz pulse imaging data. Fluct Noise Lett 1(2):L65–L70
3. Ferguson B, Wang S, Zhong H, Abbott D, Zhang XC (2003) Powder retection with T-ray imaging. Proc SPIE Terahertz Mil Secur Appl 5070:7–16
4. Fukunaga K, Hummels DM (1989) Leave-one-out procedures for nonparametric error estimates. IEEE Trans Pattern Anal Mach Intell II(4):421–423
5. Löffler T, Siebert K, Czasch S, Bauer H Tand Roskos (2002) Visualization and classification in biomedical terahertz pulsed imaging. Phys Med Biol 47(2002):3847–3852
6. Mallat SG (1999) A wavelet tour of signal processing. Academic, San Diego
7. Mittleman D, Gupta M, Neelamani R, Baraniuk G, Rudd V, Koch M (1999) Recent advances in terahertz imaging. Appl Phys B Lasers Opt 68:1085–1094
8. Qian S (2002) Time-frequency and wavelet transforms, 1st edn. Prentice Hall, Inc., New Jersey
9. Schürmann J (1996) Pattern classification: a unified view of statistical and neural approaches. Wiley, New York